Daughaday, W. H., Hall, K., Raben, M. S., Salmon, W. D., Van den Brande, J. L., & Van Wyck, J. J. (1972) *Nature 235*, 107.
Donnelly, R. A., & Rogers, J. W. (1988) *Int. J. Quantum Chem., Quantum Chem. Symp. 22*, 507–513.
Donnelly, R. A., & Rogers, J. W. (1989) *J. Opt. Theory Appl. 61*, 111–121.
Drobny, G., Pines, A., Sinton, S., Weitkamp, D. P., & Wemmer, D. (1979) *Faraday Symp. Chem. Soc. 13*, 49–55.
Dulak, N., & Temin, H. J. (1973) *J. Cell. Physiol. 81*, 153–160.
Froesch, E. R., Burgi, H., Ramseier, E. B., Bally, P., & Labhart, A. (1963) *J. Clin. Invest. 42*, 1816–1834.
Froesch, E. R., Schmid, C., Schwander, J., & Zapf, J. (1985) *Annu. Rev. Physiol. 47*, 443–467.
James, R., & Bradshaw, R. A. (1984) *Annu. Rev. Biochem. 53*, 259–292.
Jeener, J., Meier, B. H., Bachmann, P., & Ernst, R. R. (1979) *J. Chem. Phys. 71*, 4546–4553.
Maly, P., & Luthi, C. (1988) *J. Biol. Chem. 263*, 7068–7072.
Massague, J., & Czech, M. P. (1982) *J. Biol. Chem. 257*, 5038–5045.
Morgan, D. O., Edman, J. C., Standring, D. N., Fried, V. A., Smith, M. S., Roth, R. A., & Rutter, W. J. (1987) *Nature 329*, 301–307.
Nilges, M., Clore, G. M., & Gronenborn, A. M. (1987) *FEBS Lett. 219*, 11–16.
Piantini, U., Sorensen, O. W., & Ernst, R. R. (1982) *J. Am. Chem. Soc. 104*, 6800–6801.
Pullen, R. A., Lindsay, D. G., Wood, S. P., Tickle, I. J., Blundell, T. L., Wollmer, A., Krail, G., Brandenburg, D., Zahn, H., Gliemann, J., & Gammeltoft, S. (1976) *Nature 259*, 369–373.
Rechler, M. M., & Nissley, S. P. (1985) *Annu. Rev. Physiol. 47*, 425–442.
Rinderknecht, E., & Humbel, R. E. (1976) *Proc. Natl. Acad. Sci. U.S.A. 73*, 4379–4381.
Rinderknecht, E., & Humbel, R. E. (1978a) *J. Biol. Chem. 253*, 2769–2776.
Rinderknecht, E., & Humbel, R. E. (1978b) *FEBS Lett. 89*, 283–286.
Ryckaert, J. P., Cicotti, G., & Berendsen, H. J. C. (1977) *J. Comput. Physics 23*, 327–341.
Szabo, L., Mottershead, D. G., Ballard, F. J., & Wallace, J. C. (1988) *Biochem. Biophys. Res. Commun. 151*, 207–214.
Tally, M., Enberg, G., Li, C. H., & Hall, K. (1987) *Biochem. Biophys. Res. Commun. 147*, 1206–1212.
van Gunsteren, W. F., & Berendsen, H. J. C. (1977) *Mol. Phys. 34*, 1311–1327.
van Gunsteren, W. F., & Berendsen, H. J. C. (1987) *Groningen Molecular Simulation (GROMOS) Library Manual*, Biomos, Nijenborgh 16, Groningen, The Netherlands.
Wuthrich, K., Billeter, M., & Braun, W. (1984) *J. Mol. Biol. 180*, 715–740.
Yarden, Y., & Ullrich, A. (1988) *Annu. Rev. Biochem. 57*, 443–478.

Interaction of Influenza Hemagglutinin Amino-Terminal Peptide with Phospholipid Vesicles: A Fluorescence Study

Michael J. Clague,*,‡ Jay R. Knutson,§ Robert Blumenthal,‡ and Andreas Herrmann‖
Section of Membrane Structure and Function, National Cancer Institute, and Laboratory of Cell Biology, National Heart, Lung, and Blood Institute, National Institutes of Health, Bethesda, Maryland 20892, and Humboldt-Universität, Bereich Biophysik, der Sektion Biologie, Invalidenstrasse 42, 1040 Berlin, Germany

Received October 30, 1990; Revised Manuscript Received March 4, 1991

ABSTRACT: We have studied tryptophan fluorescence from a 20-residue synthetic peptide corresponding to the amino terminal of the HA2 subunit of the influenza virus hemagglutinin protein, a putative "fusion" peptide. Decay-associated spectra have been obtained at pH 7.4 and at pH 5 (the optimal pH for influenza virus fusion) in the presence and absence of liposomes. We demonstrate that a blue shift in the total steady-state fluorescence spectrum upon binding to liposomes is due to a movement in characteristic emission wavelength and increased lifetime of one of the resolved spectral components. In contrast, a further shift after lowering the pH is the product of a redistribution in the relative amplitudes of spectral components. Also, each decay component is quenched by spin-labels or anthroxyl groups normally located within the hydrocarbon interior of the membranes. Calculations are presented leading to an estimate of the distance of the tryptophan residue from the bilayer center, suggesting that the tryptophan residues are at or near the hydrocarbon–polar interface. No gross positional change was detected between pH values. Rotational depolarization is shown to be retarded by liposome binding, more so at low pH.

The induction of fusion between influenza virus and target cell membranes upon lowering of the pH has been ascribed to a conformational change of the hemagglutinin (HA)[1] spike glycoprotein, the predominant protein on the viral surface (Skehel et al., 1982). One consequence of this structural rearrangement is the exposure of the amino-terminal segment of the HA-2 subunit (White & Wilson, 1987), which, because of its hydrophobic character, is an attractive candidate for involvement in the interaction with target membranes. In order

* Address correspondence to this author at the European Molecular Biology Laboratory, Postfach 10.2209, Meyerhofstrasse 1, D-6900 Heidelberg, Federal Republic of Germany.
‡ National Cancer Institute.
§ National Heart, Lung, and Blood Institute.
‖ Humboldt-Universität.

[1] Abbreviations: BHA, hemagglutinin, bromelain fragment; DAS, decay-associated spectra; DMPC, dimyristoylphosphatidylcholine; DPPC, dipalmitoylphosphatidylcholine; HA, hemagglutinin.

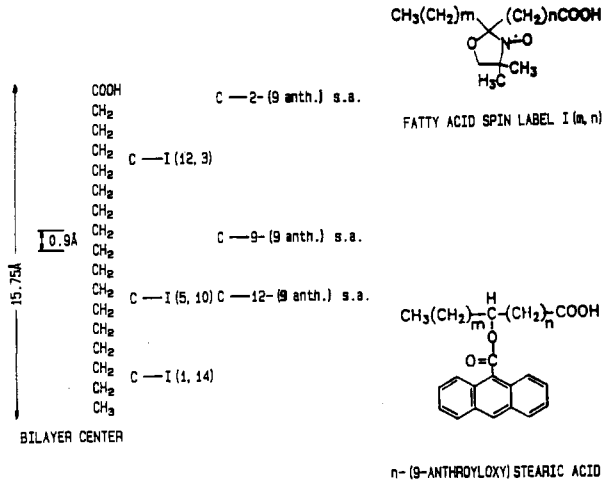

FIGURE 1: Structure and position assumed relative to the bilayer center at pH 7.4 for membrane-incorporated quenching moieties used in this study. Depth values are taken from Chattopadhyay and London (1987).

to separate characteristics of this interaction from those of a complex biological system, it is useful to study models comprising lipid membranes and synthetic peptides based upon the HA-2 amino-terminal sequence.

A number of groups have used this approach; it is now established that peptides of this type undergo a change in secondary structure upon interaction with liposomes, becoming more α-helical (Wharton et al., 1988; Murata et al., 1987a; Lear & de Grado, 1987). Moreover, the peptides alone are suffcient to promote fusion between liposomes, which under favorable conditions even occurs at neutral pH. Despite efforts to simplify, the disposition of such peptides in the membrane is difficult to determine. Duzgunes and Gambale (1988) have shown conductance changes in Montal–Muller planar membranes and release of contents from liposomes after application of heptapeptides, but not for longer sequences. Lear and De Grado show a blue shift in tryptophan fluorescence (usually indicative of a more hydrophobic environment) for 16 and 20 amino acid peptides interacting with egg lecithin liposomes. This shift is enhanced by pH reduction. Harter et al. (1989), using the water-soluble ectodomain of HA (BHA), prepared by bromelain cleavage, have shown that every third residue of this segment is labeled by a photoaffinity reagent incorporated into a target membrane, consistent with penetration normal to the membrane only as an oligomer. Brunner (1989) has extended this work to show that only probe residing in the outer membrane leaflet is capable of labeling, a result which would seem to rule out a membrane-spanning conformation, at least when the peptide is constrained by attachment to BHA.

In this study, we have used a battery of fluorescence techniques to further characterize the interaction between a peptide comprising the first 20 residues of the "B" strain of influenza virus (Gly-Phe-Phe-Gly-Ala-Ile-Ala-Gly-Phe-Leu-Glu-Gly-Gly-Trp-Glu-Gly-Met-Ile-Ala-Gly) and liposomes, with particular emphasis on the insertion problem. We have measured tryptophan fluorescence as a function of the presence of depth-dependent quenchers (Figure 1) (Chattopadhyay & London, 1987; Kleinfeld & Lukacovic, 1985; Blatt & Sawyer, 1985), and also recorded decay-associated spectra (DAS) under various conditions. Measurements which allow resolution of spectra associated with component lifetimes help constrain the interpretation of steady-state data.

Materials and Methods

Materials. A synthetic peptide corresponding to the first 20 residues of the amino-terminal segment of HA-2, influenza "B" strain, was kindly provided by W. De Grado (Du Pont). The synthetic route has been described elsewhere (Lear & De Grado, 1987). Phospholipids, 1-palmitoyl-2-(4-doxylpentanoyl)-PS, PE, and PC, spin-labeled at the 0,2-position, were provided by P. F. Devaux (Paris). Phosphatidylcholine (egg), phosphatidylserine (bovine brain), and phosphatidylethanolamine (bovine liver) were purchased from Avanti. Spin-labeled fatty acids, [5-doxylstearic acid, I(12,3), 12-doxylstearic acid, I(5,10), and 16-doxylstearic acid, I(1,14)] and fluorescent fatty acids [2,9,12-(9-anthroyloxy)stearic acid] were purchased from Molecular Probes. See Figure 1 for structures of the probes used and the position of their quenching moieties with respect to the bilayer center.

Preparation of Liposomes. Lipids dissolved in chloroform (10 mg/mL) were combined in a glass vial to give the desired final composition. Spin-labels and anthroyloxy fatty acids were also included at this stage, at concentrations of 10 and 2.5 mol %, respectively. The mixture was dried under a stream of nitrogen and then hydrated by the addition of phosphate-buffered saline (PBS) solution, typically to a concentration of 10 mg/mL. The solution was frozen and thawed 5 times before passage, 10 times under pressure, through two 0.1-μm polycarbonate filters (Nucleopore) contained within an extrusion device. The resultant liposomes have been shown to be a homogeneous unilamellar population of average diameter 90 nm (Mayer et al., 1985) Incorporation and concentration of spin-labels were checked by ESR line analysis; 2–3% of the total fatty acid spin-label is free in the aqueous medium. HA peptide was added to a vortexing lipid suspension by injection of a 1 mg/mL stock solution dissolved in dimethyl sulfoxide.

Depth-Dependent Quenching. Steady-state fluorescence spectra were recorded with an SLM8000 spectrofluorometer. The differences in quenching of tryptophan fluorescence as a function of fatty acid spin-label position were related to fluorophore depth by using the parallax formalism developed by Chattopadhyay and London (1987). For different samples containing equal concentrations of quencher at different depths, using 1 and 2 as subscripts denoting the shallower and deeper quenchers, respectively, the ratio of fluorescence intensities, F, is related to the difference in shallow quencher and fluorophore depth, z_{1F}, by

$$z_{1F} = \frac{(1/-\pi C)\ln (F_1/F_2) - L_{21}^2}{2L_{21}} \quad (1)$$

where L_{21} is the difference of the two quenchers in depth and C the concentration of each in molecules per unit area (mole fraction of quencher lipid/70 Å^2). Once z_{1F} is known, the fluorophore distance from the center of the bilayer can be calculated from

$$z_{cF} = z_{1F} + L_{c1} \quad (2)$$

where L_{c1} is the distance from the center of the bilayer to the shallow quencher.

For the deepest quencher used, spin-labeled at the 1,14-position, it is necessary to correct for quenching by quencher in the opposite leaflet of the bilayer to that in which the fluorophore is located. The equation used is then

$$z_{1F} = -2L_{21} - 2L_{c2} \pm \sqrt{\frac{-1}{\pi C}\ln\frac{F_1}{F_2} + 2L_{21}^2 + 4L_{21}L_{c2} + R_c^2} \quad (3)$$

where L_{c2} is the distance from the center of the bilayer to the deep quencher and R_c is the critical separation below which quenching occurs (~12 Å; Chattopadhyay & London, 1987).

The depth of resolved lifetime components was calculated by using the same formulas but substituting fluorescence lifetimes (derived from DAS measurements) for intensities.

Decay-Associated Spectra. Decay-associated spectra (Knutson et al., 1982) were obtained from global analysis of decay curves taken at 5-nm intervals across the emission band, using a laser-based instrument which has been described elsewhere (Knutson, 1988). Basically, a synchronously pumped, cavity-dumped dye laser provides a pulse of width <20 ps at 295 nm, with a repetition rate of 4 MHz. Vertically polarized UV pulses are obtained by frequency doubling of horizontally polarized dye laser pulses, obtained via passage through a Babinet–Soleit compensator. A vertical symmetry axis is established, and, hence, all total intensity decay measurements were obtained through an emission sheet polarizer oriented 55° from that axis ("magic angle", Badea & Brand, 1979). Emission was selected by computer-controlled JYH10 monochromators with the bandwidth set at 8 mm and a 3-mm glass slide added to further reject stray excitation. Decay curves were recorded by single-photon counting using Ortec NIM modules and a Tracor Northern multichannel analyzer under computer control. Data were transferred to a HP1000:A900 minicomputer for subsequent global analysis (Knutson et al., 1983).

Time-Resolved Anisotropy Measurements. Separate decay curves were recorded as above, for emission oriented parallel and perpendicular to the plane of excitation, by rotating a sheet polarizer. Time per channel was 88 ps, and typically 512 channels were used. By use of the minicomputer, the difference curve and the total intensity curve are combined to give the anisotropy decay curve given by

$$r(t) = \frac{I_{\parallel}(t) - I_{\perp}(t)}{I_{\parallel}(t) + 2I_{\perp}(t)} \qquad (4)$$

where $I_{\parallel}$ and I_{p}rp are emission intensities measured parallel and perpendicular to the plane of excitation, respectively. Our R955 photomultiplier operated with a time spread (half-width) of ca. 900 ps; with rigorous color correction, this arrangement can resolve lifetimes as short as 100 ps, while below that range, a faster detector is required. We used melatonin as a color shift "standard" when necessary, but frequently compensated for scattering or color shift artifacts by introducing a small fixed-lifetime component (<100 ps). This method has been shown to be as effective as more rigorous corrections when the fixed lifetime is much less than the width of the instrument response function (Knutson, 1987).

Results

Steady-State Fluorescence Associated with Binding at High and Low pH. Upon titration of egg PC liposomes into a solution containing HA-2 peptide, the steady-state intensity of tryptophan fluorescence increases, and the spectrum is blue-shifted. At lipid:peptide ratios >100:1, further changes become minimal. Similar results were obtained with DMPC and with DPPC vesicles. Binding at pH 5 gave a further blue shift and increase in fluorescence, but the shape of the binding curve was essentially the same. This low pH induced fluorescence intensity increase, observed with each lipid system, followed the relative order DPPC > DMPC > egg PC. All subsequent studies using liposomes were performed at a lipid:peptide ratio of 150:1. A noteworthy characteristic is our finding that spectral changes associated with pH 5 conditions can readily be reversed, by restoration of the pH to 7.4, and that this change is complete within our minimum time resolution (about 3 s for complete mixing).

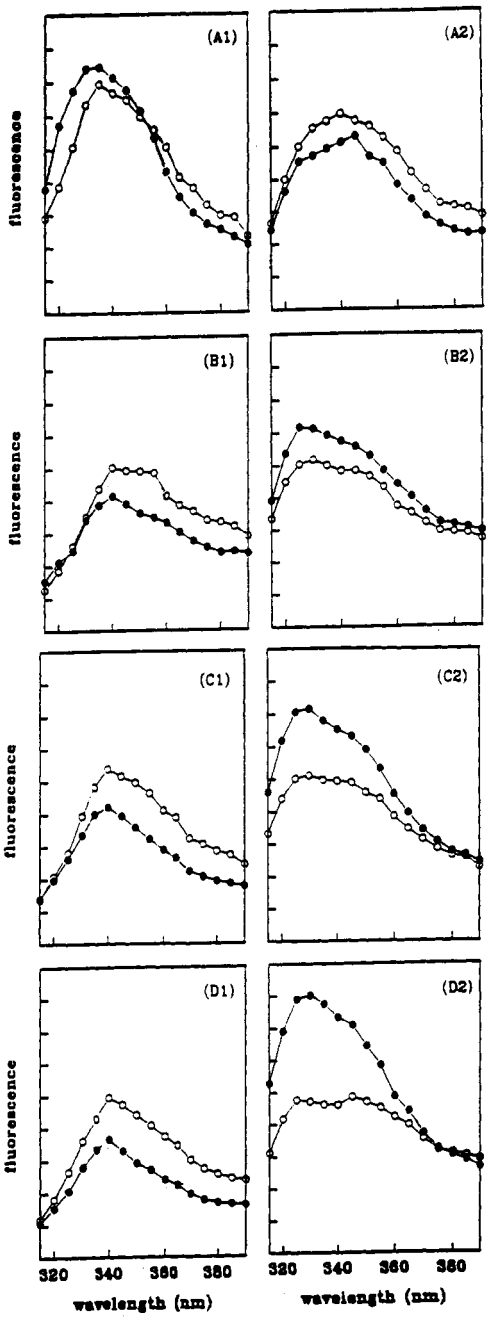

FIGURE 2: Decay-associated spectra, normalized to the same total fluorescence intensity, for peptide (A) in solution and bound to (B) egg PC, (C) DMPC and (D) DPPC; lipid:peptide ratio = 150; peptide concentration 1 μM; temperature 37 °C. Open circles, pH 7.4; filled circles, pH 5. Amplitudes and lifetimes are given in Table I. Spectra associated with τ_1 and τ_2 are designated 1 and 2, respectively, in each system.

Decay-Associated Spectra. Decay-associated spectra for peptides in solution and bound to liposomes are shown in Figure 2. By definition, DAS are the spectra associated with a particular decay function, usually an exponential. Probes in homogeneous environments (or well-spaced heterogeneous systems) provide wavelength-independent lifetimes. This is discussed more fully in Knutson et al. (1982) and references cited therein. The data for all systems were consistent in best fitting to three associated lifetimes of similar magnitudes (<1.5, 2.5–5, and >10 ns). The >10-ns lifetime component, while displaying a spectrum consistent with tryptophan (λ_{max} = 350 nm in solution), is unusually long-lived. Although it accounts for only ~4% of emitting fluorophores (see Table I), this translates into >30% of the total emission evident in a steady-state spectrum, by virtue of its long duration. For-

Table I: Associated Fluorescence Lifetimes (in Nanoseconds) of HA Peptide Measured at 37 °C in Solution and Bound to Liposomes of the Specified Composition[a]

	% α_1	τ_1	% α_2	τ_2	% α_3	τ_3
egg PC, pH 7.4	72.4	1.38	23.7	4.62	3.9	22.8
egg PC, pH 5	65.5	1.31	30.0	4.44	4.5	21.1
DMPC, pH 7.4	74.3	1.31	21.7	4.79	4.0	23.0
DMPC, pH 5	64.8	1.22	30.5	3.96	4.7	21.2
DPPC, pH 7.4	71.5	1.14	24.3	4.2	4.3	20.1
DPPC, pH 5	60.6	1.07	34.5	4.3	4.9	18.3
solution, pH 7.4	69.2	1.18	28.2	2.88	2.7	14.3
solution, pH 5	74.8	1.15	21.9	3.23	3.4	14.9

[a] Excitation was at 295 nm; decay profiles were obtained at 5-nm intervals between 315- and 395-nm emission wavelength. Corresponding fluorescence intensity spectra are shown in Figure 2. α_i is the amplitude of lifetime τ_i.

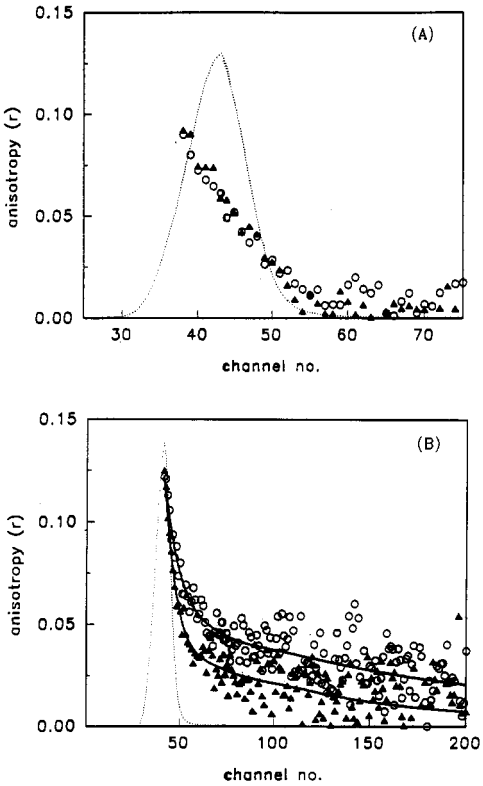

FIGURE 3: Anisotropy decays for influenza fusion peptide (A) in solution and (B) bound to LUVs composed of egg PC, lipid:protein ratio was 150:1, peptide concentration 1 μM. Excitation wavelength = 295 nm, emission wavelength = 350 nm, temperature was 40 °C. The dotted line is the lamp profile; solid lines are best-fit curves. pH was 7.4 (closed triangles) or 5.0 (open circles). 1 channel = 88 ps. Fitted rotational correlation times are given in Table II.

tunately, its total fluorescence yield remains roughly constant with reduction of pH, as do the emission wavelength characteristics, and thus it is not a source of the observed spectral changes. In fact, the major change upon reducing the pH is in the relative proportions of short- and medium-lifetime components. For each lipid system, on going from pH 7.4 to 5.0, about 6.5–10% of total fluorophores "convert" from short to medium lifetime (Table I). The concomitant increase in lifetime amplifies this effect when the normalized intensity of fluorescence is plotted (Figure 2). As this paper focuses on these two lifetime components, we subsequently refer to the <1.5-ns lifetime as short and the 2.5–5-ns lifetime as long. In solution, low pH promotes the short-lifetime component (Table I).

Time-Resolved Fluorescence Anisotropy Measurements. Measurements made at 350 nm in solution indicate a high degree of rotational freedom, consistent with a lack of secondary structure, at both pH 7.4 and pH 5. The data in both cases (Figure 3) can be fitted to a single relaxation time of ~250 ps. This is too short to reflect a global rotation of the peptide, so it must therefore be assigned to more "local segmental" motion. In the presence of liposomes, the tryptophan still possesses substantial rotational freedom. The data fit adequately to biexponential anisotropy decay curves. Reduction of the pH to 5.0 slows each component (except ϕ_1, DPPC, Table II, Figure 3), but primarily increases the amplitude of only the slower component.

Table II: Rotational Correlation Times Derived from Best Fits to Data Shown in Figure 3[a]

	β_1	ϕ_1	β_2	ϕ_2
egg PC, pH 7.4	0.082	0.45	0.038	7.96
egg PC, pH 5	0.066	0.74	0.052	14.7
DMPC, pH 7.4	0.052	0.28	0.052	5.37
DMPC, pH 5	0.03	0.92	0.062	11.1
DPPC, pH 7.4	0.135	0.25	0.044	8.71
DPPC, pH 5	0.059	0.165	0.078	12.0

[a] β_i is the amplitude for rotational correlation time ϕ_i.

Table III: Associated Fluorescence Lifetimes of HA Peptide Measured at 37 °C ($\tau_{av} = \sum\alpha_i\tau_i^2/\sum\alpha_i\tau_i$ Is the Intensity Weighted Average Lifetime Calculated from These Values)[a]

spin-label	% α_1	τ_1	% α_2	τ_2	% α_3	τ_3	τ_{av}
none, pH 7.4	72.4	1.38	23.7	4.62	3.9	22.8	8.95
none, pH 5	65.5	1.31	30.0	4.44	4.5	22.1	9.11
1,14, pH 7.4	60.8	0.91	34.1	2.95	5.1	10.8	4.46
1,14, pH 5	57.5	0.73	36.5	2.45	5.9	8.5	3.72
5,10, pH 7.4	67.6	1.00	28.2	3.35	4.3	12.5	4.89
5,10 pH 5	65.4	0.84	30.4	2.85	4.2	9.4	3.66
12,3, pH 7.4	68.4	1.01	28.2	3.44	3.4	13.6	4.86
12,3, pH 5	63.7	0.77	31.9	2.98	4.4	11.3	4.55

[a] Egg PC vesicles containing 10 mol % specified fatty acid spin-label, lipid:peptide ratio = 150. Excitation was at 295 nm; decay profiles were obtained at 4-nm intervals between 320- and 410-nm emission wavelength. α_i is the amplitude of lifetime τ_i.

Table IV: Distance from the Center of the Bilayer Calculated for Associated Lifetime Components (τ_i) Measured in the Presence of Spin-Labeled Quenchers at Different Depths in the Membrane, As Described under Materials and Methods[a]

pair of fatty acid spin-labels	distance from bilayer center (Å) at pH 7.4 τ_1	pH 7.4 τ_2	pH 5.0 τ_1	pH 5.0 τ_2
I(12,3)/I(5,10)	8.8	8.5	7.8 (9.6)	5.4 (7.2)
I(12,3)/I(1,14)	8.0	7.7	7.2 (8.3)	6.3 (7.4)
I(5,10)/I(1,14)	7.6	7.3	6.8 (7.6)	6.7 (7.5)

[a] Trans quenching has been assumed for the (1,14, label). Corrections of 2.8 and 1 Å (figures in parentheses) nearer the bilayer center have been made for quencher position at pH 5 (see text).

Depth Dependence of Quenching. Spin-label quenchers, located at three different depths (Figure 1) within the bilayer of egg PC vesicles, all cause a decrease in tryptophan fluorescence intensity (at pH 7.4). Total intensity was further reduced by reduction of the pH to 5.0. DAS measurements showed that each lifetime component is quenched to a similar extent (Table III). This actually indicates a higher efficiency of quenching for the short-lifetime component (see Discussion). The results of fluorophore depth calculations for both lifetime components are given in Table IV for three paired data sets. We have used the values for probe distances from the bilayer center assumed by Chattopadhyay and London (1987) at pH 7.4 (Figure 1). If we increase these values such that the carboxyl group is at the same depth as the lipid phosphate group, we get wildly variant values from different pairs of spin-labels. Barratt and Laggner (1974) have shown fatty acid

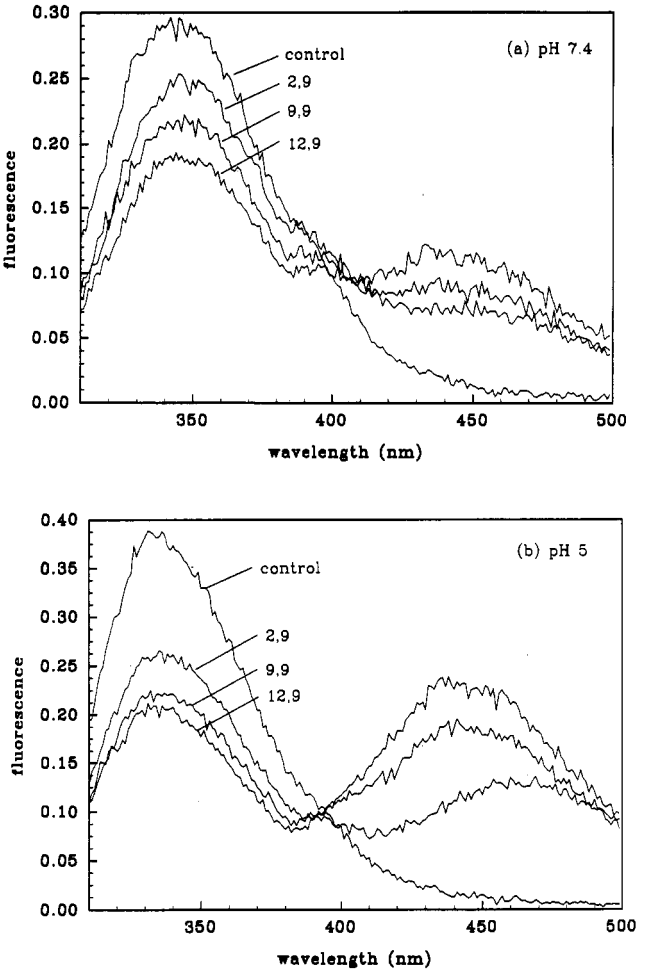

FIGURE 4: Total fluorescence spectra for egg PC liposomes containing *n*-(9-anthroyloxy)stearic acid (2.5 mol %) and having HA peptide bound, lipid:peptide ratio = 150. Temperature was 37 °C; excitation wavelength = 280 nm.

spin-labels to experience a more fluid environment upon reduction of pH, consistent with movement toward the bilayer center upon protonation of the carboxyl group. The magnitude of this movement is ill-defined. In Table IV, we show depth estimates at pH 5 assuming a movement of 2.8 Å (or 1.0 Å) toward the bilayer center for each spin-label. It is evident that the calculated position for the tryptophan residue at pH 5 is sensitive to the value assigned to spin-label movement with pH. We can only conclude that we detect no gross positional change (i.e., >3 Å) of the tryptophan between pH 7.4 and 5. Two other important features are insensitive to our spin-label depth estimates: (i) both lifetime components are at approximately the same depth; (ii) the component spectra, at both high and low pH, are essentially similar in shape to that seen with pure egg PC vesicles. Calculations from steady-state intensity measurements (data not shown) also gave depth values falling within the same range as those derived from DAS at a number of pH values between 7.4 and 5. In this case, static quenching is also included, which lifetime measurements alone are blind to.

Quenching of tryptophan fluorescence by anthroyloxy fatty acids provides a qualitatively similar result (Figure 4). An estimate of the surface potential introduced by the fluorescent fatty acids (2.5 mol %) indicates it to be an order of magnitude less than the spin-labeled fatty acids (10 mol %) at pH 7.4, 37 °C. It is therefore unlikely that pH-induced changes in the surface potential are an important factor in the observed behavior. An increase in sensitized emission is observed with

Table V: Quenching Data for HA Peptide Bound to Egg PC Liposomes Containing 10 mol % PE and PS[a]

spin-labeled phospholipid	pH	$I_{control}/I_{spin\text{-}label}$
(0,2) PC	7.4	1.37
	5.0	1.58
(0,2) PE	7.4	1.46
	5.0	1.67
(0,2) PS	7.4	1.50
	5.0	1.81

[a] 10 mol % 1-palmitoyl-2-(4-doxylpentanoyl)-PC, -PE, and -PS spin-labeled at the 0,2-position have been sequentially substituted. Lipid:peptide ratio = 150; excitation wavelength = 280 nm; emission wavelength = 350 nm; temperature = 37 °C. Results shown are the product of two experiments, both agreeing closely. $I_{control}$ and $I_{spin\text{-}label}$ represent fluorescence intensities in the absence and presence of spin-labels, respectively.

increased quenching. This demonstrates that the effect is not an artifact of changes in the tryptophan quantum yield. A quantitative evaluation of sensitized emission was not undertaken because of uncertainties relating to the quantum yield of each anthroyloxy fatty acid. Tryptophan fluorescence quenching by the aqueous quencher potassium iodide was also observed (data not shown); this was insensitive to changes in pH.

Lipid Headgroup Specificity. We examined the issue of specificity in lipid–peptide interactions as determined by phospholipid headgroup. For this, we measured the quenching of tryptophan fluorescence by PC, PE, and PS, spin-labeled at the 0,2-position, which were appropriately substituted in vesicles containing 80% PC, 10% PE, and 10% PS. To our surprise, we found that at pH 7.4 quenching efficiency decreased in the order PS = PE > PC, and at pH 5.0, PS > PE > PC (Table V).

DISCUSSION

Our binding results confirm and extend the previous fluorescence study of Lear and De Grado (1987). The binding curves are not significantly changed between pH 7.4 and 5, in accord with observations on BHA, for which it was shown that, once having undergone the low pH induced exposure of the amino terminus, it would then associate with liposomes at pH 7.4 (Doms et al., 1985). The binding results contrast the influenza peptide with another pH-dependent membrane-destabilizing peptide, the GALA peptide described by Subbarao et al. (1987), for which no binding was apparent at pH 7.4. This difference in behavior can be accounted for by the relative hydrophobicities of the two peptides (relative to each other and to themselves at different pH values). Table VI shows the results of calculations of the averaged hydrophobicities for the protonated and unprotonated forms of these peptides using scale values of Abraham and Leo (1987) based on the free energy of transferring a side chain into a hydrophobic environment. For comparison, the values obtained for presumed transmembrane sections of influenza X-31 hemagglutinin and of the well-characterized integral protein glycophorin are given. The value for the lytic peptide melittin has also been included, as this has several points of similarity with the influenza peptide, including the capacity to form an amphipathic helix and to promote fusion between liposomes (Eytan & Almary, 1983). From the table, it is evident that the unprotonated form of the fusion peptide is unlikely to span the membrane. The hydrophobicity value for the protonated form falls at the lower end of the range characteristic of transmembrane sequences but below that for the melittin 1–19 section, for which, despite immense effort, the orientation is still controversial. However, sitting stably in a membrane is

Table VI: Hydrophobicity and Hydrophobic Moments (Assuming α-Helical Structure) of Influenza Fusion Peptide, GALA Peptide, and Other Reference Sequences, Calculated According to Eisenberg (1984)[a]

peptide	av hydrophobicity	av hydrophobic moment
melittin (apis mellif. dorsata)		
whole sequence (26 AA)	0.48	0.63
19 AA of NH-terminus	1.18	0.65
glycophorin		
membrane-spanning part	1.51	0.19
fusion peptide B/Lee/40		
Glu COO(-)	0.53	0.71
Glu (COOH)	1.01	0.20
GALA peptide		
Glu COO(-)	-0.27	0.71
Glu COOH	0.87	0.20
HA2 of influenza X-31		
membrane-spanning part	1.75	0.15

[a] Glycophorin sequence from Tomita and Marchesi (1975), influenza X-31 from Gething et al. (1980).

probably not a way to induce fusion. Brasseur et al. (1990, 1988) have recently proposed an oblique penetration of viral "fusion" sequences on the basis of energy calculations.

We emphasize that the increase in fluorescence intensity upon lowering the pH in the presence of liposomes is not a property shared in solution. Beechem and Brand (1985) review evidence that protonation reduces the fluorescence yield of free tryptophan, as we see in solution.

Our DAS results are the first indication that the pH-induced change in the fluorescence spectrum, in the presence of liposomes, is not an "ensemble" property, but rather a redistribution between preexisting states associated with different fluorescence lifetimes. We think that the similarity in shape of component spectra at high and low pH is reasonable evidence that a vastly different environment is not being experienced. We can also assert that the blue shift which results from free peptide binding to liposomes has a different foundation, namely, an increase in lifetime of τ_2 concomitant with a blue shift of the associated spectrum (Figure 2 and Table III). Similar blue shifts of steady-state tryptophan spectra have been observed for a number of biologically interesting peptides upon interaction with lipid membranes, e.g., melittin, glucagon, and PhoE signal peptide (Dufourcq & Faucon, 1977; Cavatorta et al., 1986; Killian et al., 1990). In light of the present results, it will be of interest to see how these are separated into component spectra.

The finding that restoration of the pH from 5.0 to neutral leads to recovery of spectral properties associated with that pH coincides with the finding that reversal arrests the fusion of influenza virus with erythrocyte membranes (Stegmann et al., 1986) and of HA-expressing cells (at early time points after pH reduction; Morris et al., 1989). Reversibility also confirms that the observed spectral change is not an artifact of any fusion sequelae. Murata et al. (1987b) have demonstrated rapid pH "switching" for fusion of vesicles induced by succinylmelittin, but Lear and De Grado (1987) have shown that influenza peptide still retains some fusogenic activity at pH 7.4 using SUVs. Wharton et al. (1988) report that a similar sequence (based on the X31 strain of influenza) displays pH-dependent fusion when 50 mol % cholesterol is included in target liposomes.

Quantitative interpretation of the quenching results is undermined by several uncertainties, not the least of which is the possible disruption of probe position and orientation by the peptide. Our results nevertheless provide the best evidence to date that the fusion peptide, upon interaction with liposomes at pH 7.4, resides in positions where its tryptophan residue can gain intimacy with groups normally present in the hydrophobic core of the membrane, although Ohnishi (1985) has previously shown that 5-doxylstearate will quench some tryptophan fluorescence from the influenza HA-2 subunit associated with liposomes. Our rough estimate is that the single tryptophan is about 8 Å from the center of the bilayer and it retains that position on reducing the pH to 5.0. Jacobs and White (1989) have pointed out that a tryptophan side chain can penetrate this far without the peptide backbone entering the hydrocarbon region. This is supported by our finding that the aqueous quencher iodide is also effective.

Lear and De Grado (1987) have previously shown that this peptide is over 45% α-helical, when bound to POPC SUVs at pH 7.4, and helicity rises at lower pH. It is possible that our τ_1 and τ_2 associated components (in the membrane-bound case) represent unstructured and α-helical conformations, respectively, although one would require LUVs of egg PC to be less efficient at promoting helix. Interestingly, they find a 10% increase in helix upon pH reduction to pH 5. Our DAS results in the presence of quenchers imply that the tryptophan of both components is at about the same depth but the fact that the spectrum associated with τ_2 is blue-shifted relative to that of τ_1 indicates a more hydrophobic environment. This may be due to conformation rather than simple position in the bilayer.

An initial hypothesis, that pH alters the distribution between a membrane-inserted (quenched) and superficially bound (unquenched) species, can be discounted by DAS measurements, in the presence of spin-labels, showing that both lifetime components are quenched. This finding limits interpretation of the unquenched DAS results, without which we could have assigned such states to the long- and short-lifetime components, respectively. In contradistinction, lowering the pH promotes a blue-shifted, longer lifetime species, which has a decreased "accessibility" to the spin-label relative to the short-lifetime component, according to the Stern–Volmer equation:

$$\tau_0/\tau = 1 + k_q\tau_0[Q] \qquad (5)$$

where τ_0 and τ are lifetimes in the absence and presence of quencher, respectively, [Q] is the quencher concentration, and k_q is the effective bimolecular collisional rate constant. This effect is probably due to secondary structural elements differing between the two species. The finding that the degree of steady-state fluorescence quenching by spin-labeled phospholipids is dependent on the headgroup is intriguing, although we have not as yet resolved whether this is a dynamic or static effect. At pH 5, Stegmann et al. (1986) showed the extent of fusion with liposomes of influenza virus to vary according to composition such that PS > PS/DOPE (1:1) > DOPC/DOPE (1:1) > DOPC, which agrees with the pattern we obtain for quenching of PS > PE > PC.

The decrease in the extent of anisotropy decay observed upon binding to liposomes is consistent with immersion in a more viscous environment, together with the imposition of some angular restriction. We note the apparent variation of r_0 ($=\beta_1 + \beta_2$) in the fitted values given in Table II. This is due to imprecision of β_1 when ϕ_1 is small (less than half the pulse width); in contrast, β_2 is a relatively precise parameter that can quantify the "less mobile fraction". In order for the long correlation time, ϕ_2, to represent global motion, it would have to be occurring in an environment of viscosity 0.05–0.2 P, whereas the membrane interior should be in the 1–10-P range. Most likely, ϕ_2 still reflects motion more local to the fluorophore. Similar results have been observed for the tryptophan-containing hormones of approximately the same size,

ACTH(1–24) and glucagon in comparable circumstances (Gallay et al., 1989; Ross et al., 1981), suggestive of a common location. Further reduction in anisotropy decay after lowering the pH is traditionally explained by increased restriction of the average "cone angle" within which the tryptophan residue can wobble; the effect of this is to increase β_2 in accordance with the relationship (Lipari & Szabo, 1980)

$$\frac{\beta_2}{r_0} = \frac{(3\cos^2\theta - 1)^2}{2} \quad (6)$$

where θ is the angle between the emission transition dipole moment and the symmetry axis of the system. Another possibility to explain an increase in β_2 is a pH-induced shift between fast- and slow-rotating components (maybe due to aggregation). However, the magnitude of this change would not correlate with the observed change in distribution of fluorescence lifetime associated species.

In summary, the fusion peptide binds to liposomes in a manner such that its tryptophan residue can penetrate to within 8 Å of the bilayer center while remaining accessible to the aqueous phase. We assume that this localization enables it to promote fusion by virtue of bilayer destabilization. A dynamic equilibrium exists between two tryptophan environments displaying distinct spectral characteristics. Reduction in pH promotes the blue-shifted component, which may represent the fusogenic conformation. We can make the distinction between an altered mixture (microheterogeneity) and an ensemble property because of our resolution of the total spectrum into decay-associated spectra. We believe that similar studies could yield insight into a variety of other peptide interactions with membranes.

Acknowledgments

We thank Drs. W. De Grado and P. Devaux for gifts of peptide and spin-labeled phospholipids, respectively.

Registry No. pH, 12408-02-5.

References

Badea, M. G., & Brand, L. (1979) *Methods Enzymol. 75*, 378–425.

Barratt, M. D., & Laggner, P. (1974) *Biochim. Biophys. Acta 363*, 127–133.

Beechem, J. M., & Brand, L. (1985) *Annu. Rev. Biochem. 54*, 43–71.

Blatt, E., & Sawyer, W. H. (1985) *Biochim. Biophys. Acta 822*, 43–63.

Brasseur, R., Lorge, P., Goormaghtigh, E., Ruysschaert, J.-M., Espion, D., & Burny, A. (1988) *Virus Genes 1*, 325–332.

Brasseur, R., Vanderbranden, M., Cornet, B., Burny, A., & Ruysschaert, J.-M. (1990) *Biochim. Biophys. Acta 1029*, 267–273.

Brunner, J. (1989) *FEBS Lett. 257*, 369–373.

Cavatorta, P., Farruggia, G., Masotti, L., Sartor, G., & Szabo, A. G. (1986) *Biochem. Biophys. Res. Commun. 141*, 99–105.

Chattopadhyay, A., & London, E. (1987) *Biochemistry 26*, 39–45.

Doms, R. W., Helenius, A., & White, J. (1985) *J. Biol. Chem. 260*, 2973–2981.

Dufourcq, J., & Faucon, J. F. (1977) *Biochim. Biophys. Acta 467*, 1–11.

Duzgunes, N., & Gambale, F. (1988) *FEBS Lett. 227*, 110–114.

Eisenberg, D. (1984) *Annu. Rev. Biochem. 53*, 595–623.

Gallay, J., Vincent, M., Nicot, C., & Waks, M. (1989) in *Fluorescent Biomolecules* (Jameson, D. M., & Reinhardt, G. D., Eds.) pp 397–400, Plenum Press, New York.

Gething, M.-J., Bye, J., Skehel, J. J., & Waterfield, M. (1980) *Nature 287*, 301–306.

Harter, C., James, P., Bachi, T., Semenza, G. & Brunner, J. (1989) *J. Biol. Chem. 264*, 6459–6464.

Jacobs, R. E., & White, S. H. (1989) *Biochemistry 28*, 3421–3437.

Killian, J. A., Keller, R. C. A., Struyve, M., de Kroon, A. I. P. M., Tommassen, J., & De Kruijff, B. (1990) *Biochemistry 30*, 8131–8137.

Kleinfeld, A., & Lukacovic, M. F. (1985) *Biochemistry 24*, 1883–1890.

Knutson, J. R. (1987) *Biophys. J. 51*, 285a.

Knutson, J. R. (1988) *Proc. SPIE—Int. Soc. Opt. Eng. 909*, 51–60.

Knutson, J. R., Walbridge, D. G., & Brand, L. (1982) *Biochemistry 21*, 4671–4679.

Knutson, J. R., Beechem, J. M., & Brand, L. (1983) *Chem. Phys. Lett. 102*, 501–507.

Lear, J. D., & De Grado, W. F. (1987) *J. Biol. Chem. 262*, 6500–6505.

Lipari, G., & Szabo, A. (1980) *Biophys. J. 30*, 489–506.

Mayer, L. D., Bally, M. B., Hope, M. J., & Cullis, P. R. (1985) *Biochim. Biophys. Acta 816*, 294–302.

Morris, S. J., Sarkar, D. P., White, J. M., & Blumenthal, R. (1989) *J. Biol. Chem. 264*, 3972–3978.

Murata, M., Suguhara, Y., Takahashi, S., & Ohnishi, S. (1987a) *J. Biochem. 102*, 957–962.

Murata, M., Nagayama, K., & Ohnishi, S. (1987b) *Biochemistry 26*, 4056–4062.

Ohnishi, S. H. (1985) *Vaccine 3*, 204–205.

Ross, J. B., Rousslang, K. W., & Brand, L. (1981) *Biochemistry 20*, 4361–4369.

Skehel, J. J., Bayley, P. M., Brown, E. B., Martin, S. R., Waterfield, M. D., White, J. M., Wilson, I. A., & Wiley, D. C. (1982) *Proc. Natl. Acad. Sci. U.S.A., 79*, 968–972.

Stegmann, T., Hoekstra, D., Scherpof, G., & Wilschut, J. (1985) *Biochemistry 24*, 3107–3113.

Tomita, M., & Marchesi, V. T. (1975) *Proc. Natl. Acad. Sci. U.S.A. 72*, 2964–2968.

Wharton, S. A., Martin, S. R., Ruigrok, R. W. H., Skehel, J. J., & Wiley, D. C. (1988) *J. Gen. Virol. 69*, 1847–1857.

White, J. M., & Wilson, I. (1987) *J. Cell Biol. 105*, 2887–2896.